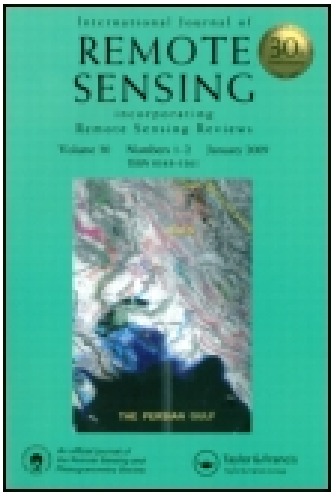

International Journal of Remote Sensing
Publication details, including instructions for authors and subscription information:
http://www.tandfonline.com/loi/tres20

Bare surface soil moisture retrieval from the synergistic use of optical and thermal infrared data

Pei Leng[ab], Xiaoning Song[a], Zhao-Liang Li[bc], Jianwei Ma[a], Fangcheng Zhou[a] & Shuang Li[a]

[a] College of Resources and Environment, University of Chinese Academy of Sciences, Beijing 100049, China

[b] ICube, UdS, CNRS, Illkirch 67412, France

[c] Key Laboratory of Agri-informatics, Ministry of Agriculture/ Institute of Agricultural Resources and Regional Planning, Chinese Academy of Agricultural Sciences, Beijing 100081, China

Published online: 03 Feb 2014.

To cite this article: Pei Leng, Xiaoning Song, Zhao-Liang Li, Jianwei Ma, Fangcheng Zhou & Shuang Li (2014) Bare surface soil moisture retrieval from the synergistic use of optical and thermal infrared data, International Journal of Remote Sensing, 35:3, 988-1003, DOI: 10.1080/01431161.2013.875237

To link to this article: http://dx.doi.org/10.1080/01431161.2013.875237

International Journal of Remote Sensing, 2014
Vol. 35, No. 3, 988–1003, http://dx.doi.org/10.1080/01431161.2013.875237

Bare surface soil moisture retrieval from the synergistic use of optical and thermal infrared data

Pei Leng[a,b], Xiaoning Song[a]*, Zhao-Liang Li[b,c], Jianwei Ma[a], Fangcheng Zhou[a], and Shuang Li[a]

[a]*College of Resources and Environment, University of Chinese Academy of Sciences, Beijing 100049, China;* [b]*ICube, UdS, CNRS, Illkirch 67412, France;* [c]*Key Laboratory of Agri-informatics, Ministry of Agriculture/Institute of Agricultural Resources and Regional Planning, Chinese Academy of Agricultural Sciences, Beijing 100081, China*

(*Received 9 April 2013; accepted 29 July 2013*)

Land surface soil moisture (SSM) is crucial to research and applications in hydrology, ecology, and meteorology. To develop a SSM retrieval model for bare soil, an elliptical relationship between diurnal cycles of land surface temperature (LST) and net surface shortwave radiation (NSSR) is described and further verified using data that were simulated with the Common Land Model (CoLM) simulation. In addition, with a stepwise linear regression, a multi-linear model is developed to retrieve daily average SSM in terms of the ellipse parameters x_0 (horizontal coordinate of the ellipse centre), y_0 (vertical coordinate of the ellipse centre), a (semi-major axis), and θ (rotation angle), which were acquired from the elliptical relationship. The retrieval model for daily average SSM proved to be independent of soil type for a given atmospheric condition. Compared with the simulated daily average SSM, the proposed model was found to be of higher accuracy. For eight cloud-free days, the root mean square error (RMSE) ranged from 0.003 to 0.031 $m^3\ m^{-3}$, while the coefficient of determination (R^2) ranged from 0.852 to 0.999. Finally, comparison and validation were conducted using simulated and measured data, respectively. The results indicated that the proposed model showed better accuracy than a recently reported model using simulated data. A simple calibration decreased RMSE from 0.088 $m^3\ m^{-3}$ to 0.051 $m^3\ m^{-3}$ at Bondville Companion site, and from 0.126 $m^3\ m^{-3}$ to 0.071 $m^3\ m^{-3}$ at the Bondville site. Coefficients of determination R^2 = 0.548 and 0.445 were achieved between the estimated daily average SSM and the measured values at the two sites, respectively. This paper suggests a promising avenue for retrieving regional SSM using LST and NSSR derived from geostationary satellites in future developments.

1. Introduction

Land surface soil moisture (SSM) content is crucial to research and applications in hydrology, ecology, and meteorology (Saha 1995; Pierdicca, Pulvirenti, and Bignami 2010). In hydrology, SSM strongly influences the transfer of water between the soil surface and the atmosphere, and it affects the water balance between the local and regional scale (Mintz and Serafini 1992; Entekhabi and Rodriquez-Iturbe 1994; Gokmen et al. 2012). In ecology, SSM is an essential parameter for various models and has a major effect on net ecosystem productivity (NEP) estimates and yield forecasts (Krishnan et al. 2006; Qian, Jong, and Gameda 2009). In climatological research, SSM is considered as a

*Corresponding author. Email:songxn@ucas.ac.cn

significant variable that can affect climate change at regional or even global scales (Szép, Mika, and Dunkel 2005; Seneviratne et al. 2010).

In the recent decades of rapid development in remote-sensing technology, many optical remote-sensing methods have been introduced to estimate SSM or SSM-related surface variables (Verstraeten et al. 2006; Song and Zhao 2006; Minacapilli, Iovino, and Blanda 2009; Patel et al. 2009; Li et al. 2009; Chen et al. 2011; Li, Tang, et al. 2013; Li, Wu, et al. 2013). However, most of these methods were originally developed with polar-orbiting remotely sensed data, including data from the Moderate Resolution Imaging Spectroradiometer (MODIS) and Advanced Very High Resolution Radiometer (AVHRR), and only limited (usually one or two) instantaneous remotely sensed images are available for a given study area over a clear-sky day using those polar-orbiting satellites, which does not benefit the long-term monitoring of SSM time series. In comparison, geostationary satellite data are used less in SSM retrieval methods, mainly because of their lower spatial resolution in comparison with polar-orbiting satellite data. However, they are capable of observing the Earth with a much higher temporal resolution (48–96 per day) with the same view angle for a given pixel. With the characteristic of stationary observation from space, geostationary satellite data are not only providing land surface information that is closely related with SSM, such as land-surface temperature (LST) and net surface shortwave radiation (NSSR), but are also capable of describing their daily evolution. Thus, they are likely to be more promising for mapping and monitoring SSM time series than polar-orbiting remotely sensed data. According to previous studies (Schmugge et al. 1978; Price 1977, 1980; Xue and Cracknell 1995; Wetzel, Atlas, and Woodward 1984; Wetzel and Woodward 1987; Zhao and Li 2013; Song et al. 2013), both multi-temporal field data and satellite-derived land-surface variables have been employed to estimate SSM. At the very beginning, the amplitude of the diurnal range of soil surface temperature was considered as a reliable indicator of soil moisture conditions (Schmugge et al. 1978). In addition, other SSM indicators for bare or sparsely vegetated areas, such as thermal inertia and apparent thermal inertia (ATI), have been calculated based on temperature variation (Price 1977, 1980). Consequently, a simplified thermal inertia model was proposed that incorporates the phase angle and the time of maximum air temperature in the diurnal temperature cycle (Xue and Cracknell 1995). However, the relationship between ATI and SSM varies with soil type. In addition to acquiring multiple surface temperature measurements, researchers have suggested combining surface temperature and the variation in absorbed solar radiation to estimate SSM, and the mid-morning difference between the surface temperature and the absorbed solar radiation has been discovered to be optimally sensitive to SSM (Wetzel, Atlas, and Woodward 1984; Wetzel and Woodward 1987). On this basis, Zhao and Li (2013) proposed a simple multi-linear model to estimate SSM with T_N (the LST increasing rate normalized by the difference in the net surface shortwave radiation at 1.5 hours and 4.5 hours after sunrise at mid-morning) and t_m (the time at which the daily maximum temperature occurs). Applying this method is limited by the ability to determine t_m and the nonlinear relationship between T_N and SSM. Therefore, Zhao et al. (2013) modified Zhao and Li's (2013) SSM retrieval model and verified it using field measurements.

In summary, for optical and thermal infrared remote sensing, most of the previous SSM retrieval studies focus on only a single daily measurement or on the mid-morning thermal infrared and optical data (Verstraeten et al. 2006; Song and Zhao 2006; Minacapilli, Iovino, and Blanda 2009; Patel et al. 2009; Chen et al. 2011; Wetzel, Atlas, and Woodward 1984; Wetzel and Woodward 1987; Zhao and Li 2013; Zhao et al. 2013). However, all-day optical and thermal infrared data are capable of providing

additional information about the underlying surface, which will probably improve SSM retrieval. This paper attempts the synergistic use of daytime thermal infrared and optical data to develop a novel and feasible retrieval model for daily average SSM, where the diurnal cycles of LST and NSSR are used. This model has significant potential for future development, given the attention that geostationary satellite-derived land-surface variables have recently been accorded (Sobrino and Romaguera 2004; Jiang, Li, and Nerry 2006; Tang et al. 2008; Lu et al. 2011; Song et al. 2013).

2. Methodology

2.1. Elliptical relationship between diurnal LST and NSSR cycles

The diurnal LST cycle can usually be described as a sine or cosine function. Based on the Diurnal Temperature Cycle (DTC) model proposed by Göttsche and Olesen (2001), Jiang, Li, and Nerry (2006) presented a modified DTC model. The daytime part of the DTC model can be written as:

$$T(t) = T_0 + T_a \cos[\beta(t - t_m)], \tag{1}$$

where $T(t)$ is the LST (K) at time t (hours), T_0 is the residual temperature at sunrise, T_a is the temperature amplitude, β is the width of the half-period of the cosine term, and t_m is the time at which the temperature reaches its maximum.

Since the diurnal LST cycle can be expressed as a cosine function of time t (hours), a similar cosine function can also be applied to describe the diurnal NSSR cycle:

$$S_n(t) = S_0 + S_a \cos[\alpha(t - t_r)], \tag{2}$$

where $S_n(t)$ is NSSR ($W\,m^{-2}$) at time t (hours), S_0 is the residual NSSR at sunrise, S_a is the NSSR amplitude, α is the width of the half-period of the cosine term, and t_r is the time (hours) of maximum NSSR.

To simplify the expression and better investigate the relationship between the diurnal LST and NSSR cycles, each variable can be modified to make it dimensionless. The dimensionless diurnal cycles of LST and NSSR are:

$$x = \frac{T(t) - s}{r - s} = p_1 \cos[\beta(t - t_m)] + q_1, \tag{3}$$

$$y = \frac{S_n(t) - j}{k - j} = p_2 \cos[\alpha(t - t_r)] + q_2, \tag{4}$$

where x is the dimensionless LST, y is the dimensionless NSSR, r and s are set as 325 K and 275 K, respectively, and k and j are set as 1200 W m^{-2} and 0, respectively, such that p_1, q_1, p_2, and q_2 are parameters of diurnal LST and NSSR cycles.

For a day of clear skies, it is assumed that β in Equation (1) is equal to α in Equation (2). If the difference between maximum LST time t_m and maximum NSSR time t_r is defined as $\Delta t(\Delta t = t_m - t_r)$, the following formula can then be derived:

$$p_2^2(x-q_1)^2-2p_1p_2[\cos(\beta\times\Delta t)](x-q_1)(y-q_2) + p_1^2(y-q_2)^2=[p_1p_2\sin(\beta\times\Delta t)]^2. \quad (5)$$

For a given atmospheric condition, p_1, q_1, p_2, q_2, β, and Δt are constants for a particular soil type and soil moisture content. Therefore, Equation (5) could be considered as an expression of an arbitrary ellipse. The ellipse parameters, including the centre horizontal coordinate (x_0), the centre vertical coordinate (y_0), the semi-major axis (a), the semi-minor axis (b), and the rotation angle (θ) can be calculated as:

$$\begin{cases} x_0 = q_1 \\ y_0 = q_2 \\ \theta = \frac{1}{2}\cot^{-1}\left[\dfrac{p_1^2-p_2^2}{2p_1p_2\cos(\beta\times\Delta t)}\right] \\ a = p_1\sin(\beta\times\Delta t) \\ b = p_2\sin(\beta\times\Delta t). \end{cases} \quad (6)$$

Clearly, the elliptical relationship would vary with different soil types and soil moisture contents for bare surface under a given atmospheric condition. There is thus an elliptical relationship between the diurnal LST and NSSR cycles.

2.2. *Experiment design and data simulation*

A database containing diurnal LST and NSSR cycles, as well as SSM under different underlying surfaces and atmospheric conditions, is needed for the methodological development of the SSM retrieval model. Although diurnal LST and NSSR cycles could be acquired from geostationary satellite data, such as the Meteosat Second Generation (MSG) with a spatial resolution of 3 km, it may not be possible to obtain the corresponding SSM at such scale with acceptable accuracy from either satellites or field measurements. Alternatively, the land-surface model, which is capable of describing the diurnal LST and NSSR cycles and the evolution of SSM with different underlying surfaces and atmospheric conditions, is used to produce all these data and construct the database for the methodology development.

The Common Land Model (CoLM) was selected to simulate the diurnal LST and NSSR cycles for different soil types and different ranges of SSM for bare surfaces. CoLM is an improved version of the Community Land Model (CLM2.0, CLM3.0 versions), and is radically different from the initial version and from CLM2.0 and CLM3.0. To date, the model performance has been validated in sites with extensive field data, including some sites adopted by the Project for Intercomparison of Land-surface Parameterization Schemes (Cabauw, Valdai, Red-Arkansas river basin) and others (First ISLSCP Field Experiment (FIFE), Boreal Ecosystem-Atmosphere Study (BOREAS), Hydrological Atmospheric Pilot Experiment – Modelisation du BiLan Hydrique (HAPEX-MOBILHY), Anglo-Brazilian Amazonian Climate Observation Study (ABRACOS), Sonoran Desert, Global Soil Wetness Project (GSWP), Land Data Assimilation Systems (LDAS)) (Dai and Ji 2008).

Figure 1 depicts the scheme of the methodology development of the SSM retrieval model. As in the flowchart, simulation is the most significant part, which directly produces data to construct the database. For the initialization of the CoLM, land-cover type was set as Barren or Sparely Vegetated according to the United States Geological

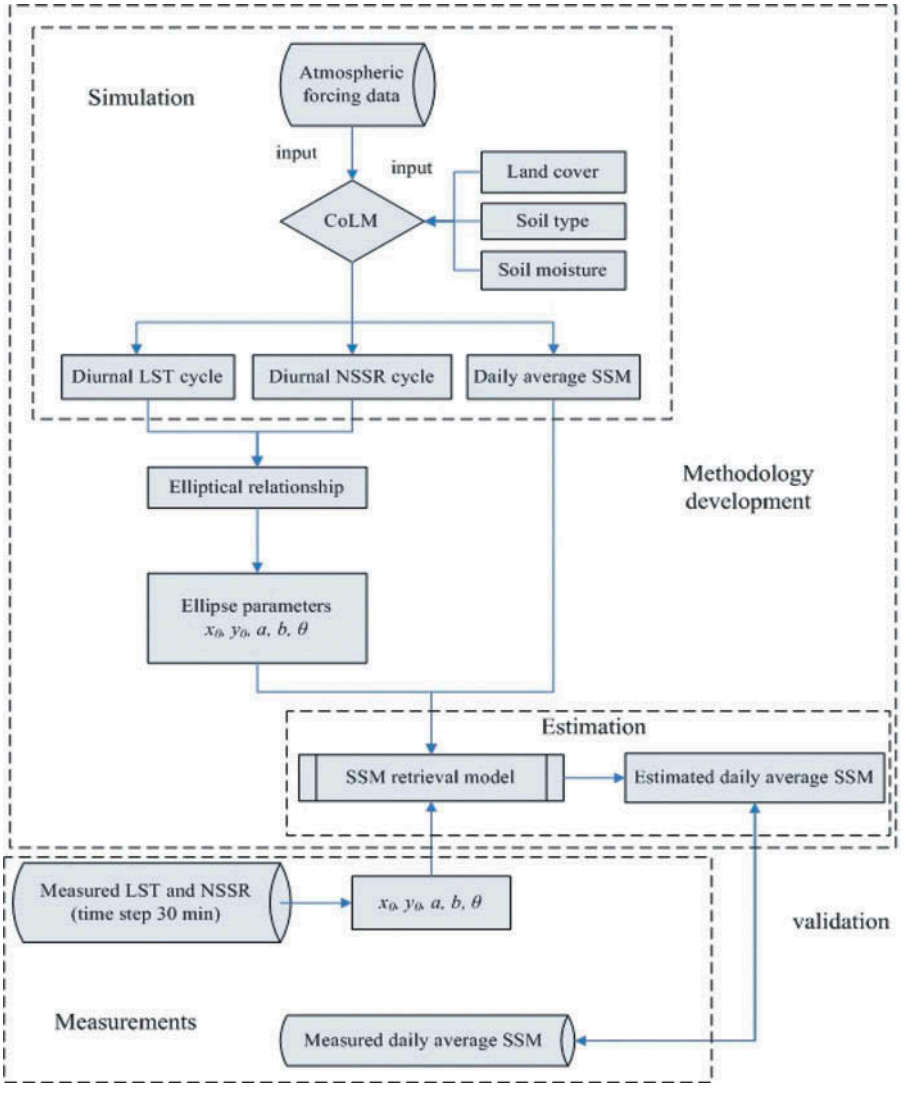

Figure 1. Scheme for methodology development of the daily average SSM retrieval model.

Survey (USGS) vegetation categories, and fractional vegetation cover was set as 0. In total, eight typical soil types and each range of soil moisture (Table 1) were also conducted in the CoLM simulation. Besides, atmospheric forcing data (Table 2) of eight cloud-free days from early April to late October in the year 2001 at the Bondville site (40.0062° N, 88.2904° W), including downward solar radiation, downward longwave radiation, precipitation, air temperature, wind speed, wind direction, atmospheric pressure at the surface, and specific humidity, were used to drive the CoLM. Finally, the LP-sampling method (Saltelli et al. 2004), integrated in GEM-SA (Gaussian Emulation Machine for Sensitivity Analysis) was used to represent eight typical soil types, eight typical atmospheric conditions, and a range of SSM values for each soil type. As LST responds to SSM at depths of 4–5 cm (Idso et al. 1975), the first soil layer of the CoLM

Table 1. Soil types and ranges of SSM used in the CoLM simulations.

No.	Sand (%)	Clay (%)	Soil types	Range of SSM (m^3 m^{-3})
1	25	50	Clay	0.05–0.421
2	10	45	Silty clay	0.05–0.409
3	10	35	Silty clay loam	0.05–0.382
4	30	35	Clay loam	0.05–0.358
5	15	20	Silty loam	0.05–0.332
6	40	20	Loam	0.05–0.280
7	50	40	Sandy clay	0.05–0.361
8	50	30	Sandy clay loam	0.05–0.309

Table 2. Primary characteristics of atmospheric conditions for the eight cloud-free days used in the CoLM simulation used to develop the daily average SSM retrieval model.

Year	DOY	Maximum solar radiation (W m^{-2})	Average wind speed (m s^{-1})	Average air temperature (K)
2001	103	864	4.05	287.68
	128	906	3.05	297.25
	167	918	3.02	303.85
	192	1035	3.46	298.95
	216	968	3.20	302.25
	248	885	2.92	302.65
	274	774	2.59	298.75
	298	694	15.50	281.39

was set to 5 cm. With the simulation, the selected outputs of the simulation mainly include diurnal LST and NSSR cycles, as well as daily average SSM.

3. Results and discussion

3.1. *Fitting ellipses with simulated data*

The elliptical relationship between the diurnal LST and NSSR cycles has been discussed above. To assess the validity of this relationship, the simulated data were fitted to the elliptical relationship using the direct least squares fitting method (Fitzgibbon, Pilu, and Fisher 1999). An example of the ellipse that fits the relationship between the diurnal LST and NSSR cycles is shown in Figure 2. Figure 3 depicts the ellipses that were fitted with different SSM values for the same soil type, while Figure 4 describes different soil types with the same SSM. It is clear from Figures 3 and 4 that the ellipse varies with different soil types and SSM values. Thus, the ellipse parameters are most likely capable of determining the SSM for various soil types under a given set of atmospheric conditions.

3.2. *Daily average SSM retrieval model*

As stated above, an elliptical relationship exists between the diurnal LST and NSSR cycles, and the elliptical relationship varies with different soil types and SSM under a given atmospheric condition. To develop the SSM retrieval model using the ellipse

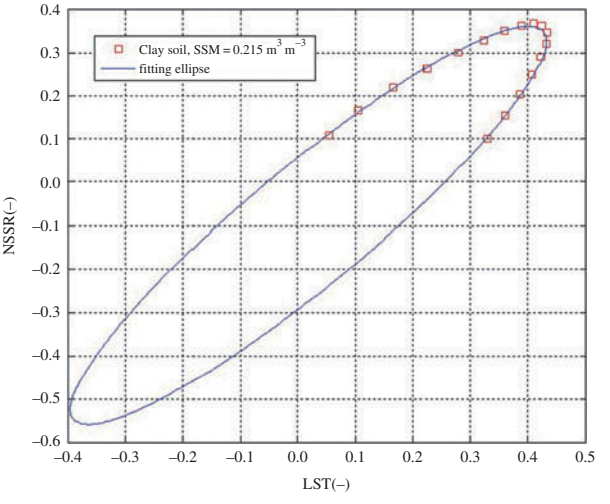

Figure 2. Ellipse fitted to the relationship between diurnal LST and NSSR cycles using simulated data for clay soil with SSM = 0.215 m^3 m^{-3} on DOY 302, 2006.

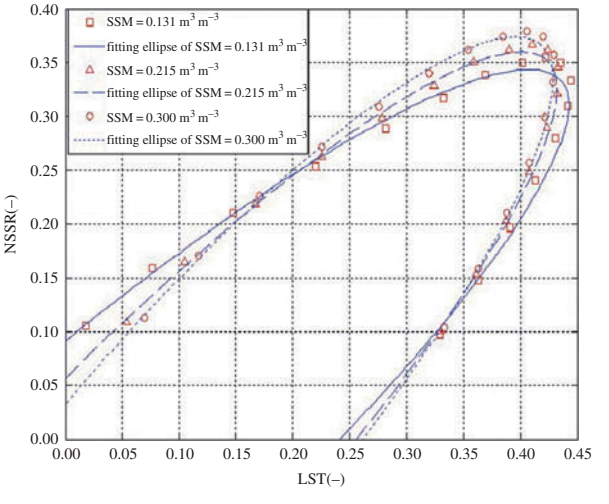

Figure 3. Ellipses fitted to the relationship between diurnal LST and NSSR cycles using simulated data for clay soil with SSM = 0.131 m^3 m^{-3}, 0.215 m^3 m^{-3}, and 0.300 m^3 m^{-3}, respectively, on DOY 302, 2006.

parameters and to eliminate the effect of soil types, correlation analysis was first conducted to analyse the relationships between the elliptical parameters. Taking the simulated data for day of year (DOY) 274 as an example, the results of correlation analysis are shown in Table 3. As shown in Table 3, the absolute value of the correlation between the four ellipse parameters, x_0, y_0, a, and b ranges from 0.898 to 0.987, which indicates quite significant correlations among them, while for the parameter θ, non-significant correlations were shown with other ellipse parameters. As most of the ellipse parameters are highly correlated to each other, and it is difficult to determine which ellipse parameters are

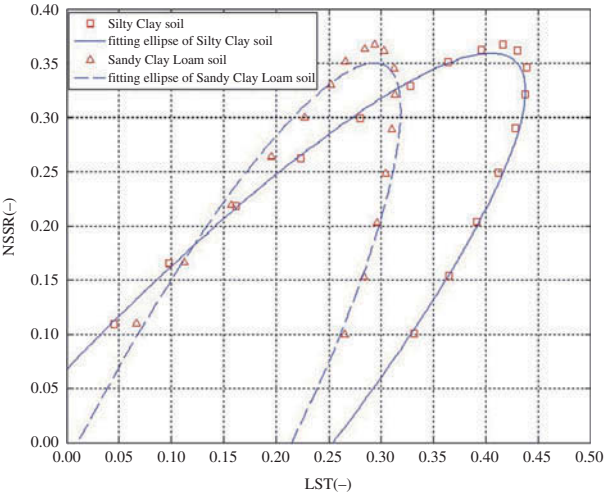

Figure 4. Ellipses fitted to the relationship between diurnal LST and NSSR cycles using simulated data for silty clay soil and sandy clay loam soil with SSM = 0.219 m^3 m^{-3} on DOY 302, 2006.

Table 3. Correlation coefficients between the ellipse parameters (DOY 274).

	x_0	y_0	a	b	θ
$\boldsymbol{x_0}$	1.000				
$\boldsymbol{y_0}$	0.987	1.000			
$\boldsymbol{a}$	–0.957	–0.984	1.000		
$\boldsymbol{b}$	–0.927	–0.944	0.898	1.000	
$\boldsymbol{\theta}$	–0.170	–0.064	–0.099	0.246	1.000

suitable to retrieve SSM, a stepwise multi-linear regression (using SSM as the dependent variable) was further performed and the five ellipse parameters (x_0, y_0, a, b, θ) were analysed as possible independent variables. It should be noted that all soil types with all their SSM simulations were used in the regression. The stepwise multi-linear regression for DOY 274 is shown as an example in Table 4.

As shown in Table 4, the three ellipse parameters (θ, y_0, a) in step 3 achieved a relatively high degree of accuracy, with RMSE = 0.024 m^3 m^{-3} and R^2 = 0.912. Further, using the four ellipse parameters (θ, y_0, a, x_0) in step 4 decreased the RMSE significantly, from 0.024 m^3 m^{-3} to approximately 0.010 m^3 m^{-3}. With additional parameters, the

Table 4. Summary of stepwise regression process using SSM and five ellipse parameters for DOY 274.

Step	Parameters	RMSE (m^3 m^{-3})	R^2
1	θ	0.045	0.694
2	θ, y_0	0.033	0.837
3	θ, y_0, a	0.024	0.912
4	θ, y_0, a, x_0	0.010	0.987
5	θ, y_0, a, x_0, b	0.009	0.990

RMSE would not have exhibited any further significant decrease. Thus a multi-linear relationship to retrieve daily average SSM in terms of the four ellipse parameters (x_0, y_0, a, θ) could be written as:

$$\mathrm{SSM} = n_1 \times x_0 + n_2 \times y_0 + n_3 \times a + n_4 \times \theta + n_0, \quad (7)$$

where SSM is the daily average SSM ($m^3\ m^{-3}$) and x_0, y_0, a, and θ are the ellipse parameters, representing the ellipse centre horizontal coordinate, ellipse centre vertical coordinate, semi-major axis, and rotation angle, respectively. n_i (i = 0, 1, 2, 3, 4) are the fitting coefficients ($m^3\ m^{-3}$).

A comparison of the estimated daily average SSM using Equation (7) and the simulated daily average SSM are shown in Figure 5. The result of the stepwise multi-linear regression contains different soil types, which means that the daily average SSM retrieval model and the model parameters n_i (i = 0, 1, 2, 3, 4) in Equation (7) are independent of soil type and are related only to the atmospheric conditions of each day.

As Figure 5 is based on the data simulated for DOY 274, to determine the general applicability of the proposed SSM retrieval model, the stepwise multi-linear regression was finally conducted on the simulated SSM data for the other seven cloud-free days, with the four ellipse parameters (x_0, y_0, a, θ) as independent variables. The results of model parameters n_i (i = 0, 1 , 2, 3, 4) of the total eight cloud-free days are presented in Table 5, and the scatter plots of the estimated daily average SSM from Equation (7) and the simulated daily average SSM for the eight cloud-free days are presented in Figure 6. According to Table 5 and Figure 6, the coefficient of determination, R^2, ranges from 0.852 to 0.999, while the RMSE ranges from 0.003 to 0.031 $m^3\ m^{-3}$. The R^2 and RMSE for all situations are 0.953 and 0.017 $m^3\ m^{-3}$, respectively, which indicates that the daily average SSM retrieval model is stable, and it is feasible to estimate daily average SSM using Equation (7) with the varying model parameters n_i (i = 0, 1, 2, 3, 4) that depend only on the atmospheric conditions for each individual cloud-free day.

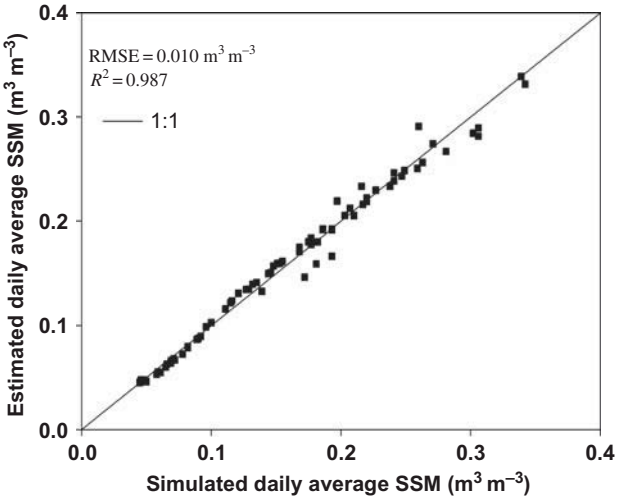

Figure 5. Comparison of daily average SSM estimated using Equation (7) with simulated average SSM for DOY 274, 2001.

Table 5. Model parameters in Equation (7) for the eight cloud-free days.

DOY	n_1	n_2	n_3	n_4	n_0	R^2	RMSE (m^3 m^{-3})
103	3.455	3.811	4.894	0.941	–4.540	0.928	0.022
128	1.467	5.351	5.146	0.674	–4.273	0.933	0.021
167	0.024	5.331	4.180	0.192	–2.889	0.991	0.008
192	–0.224	4.214	3.457	0.357	–2.637	0.999	0.003
216	–0.619	5.287	3.862	1.100	–3.440	0.852	0.031
248	1.107	1.290	1.618	0.936	–2.782	0.948	0.018
274	3.308	3.052	4.077	1.516	–4.315	0.987	0.010
298	–0.923	7.842	5.309	0.566	–2.996	0.986	0.010
Total						0.953	0.017

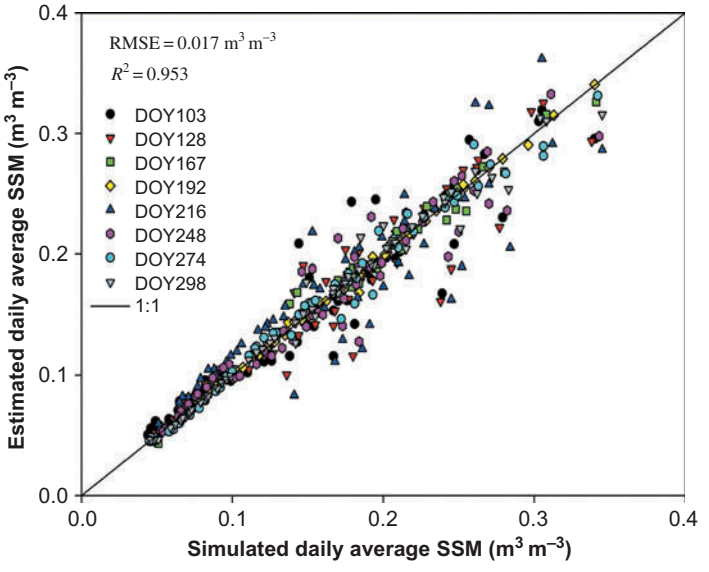

Figure 6. Comparison of daily average SSM estimated using Equation (7) with simulated average SSM for each of eight cloud-free days.

3.3. *Comparison with Zhao and Li's (2013) model*

Zhao and Li (2013) reported a multi-linear model to estimate SSM generally using two parameters T_N and t_m, which were obtained based on the mid-morning segment of diurnal LST and NSSR cycles. Since both Zhao and Li's (2013) model and the proposed SSM retrieval model are based on the evolution of LST and NSSR, a comparison between these two models was conducted to evaluate the availability of the proposed model using simulated data. First, the simulated time series of LST were used to fit the diurnal LST cycle according to Equation (1) on the eight cloud-free days to acquire the parameter t_m for each simulation. Then, both the time series LST and NSSR during the mid-morning were used to calculate the parameter T_N for each simulation. Finally, a multi-linear regression model for daily average SSM retrieval was obtained by taking the daily average SSM as the dependent variable, and T_N and t_m as the independent variables. Similarly to the model proposed in this paper, the model parameters of Zhao and Li's

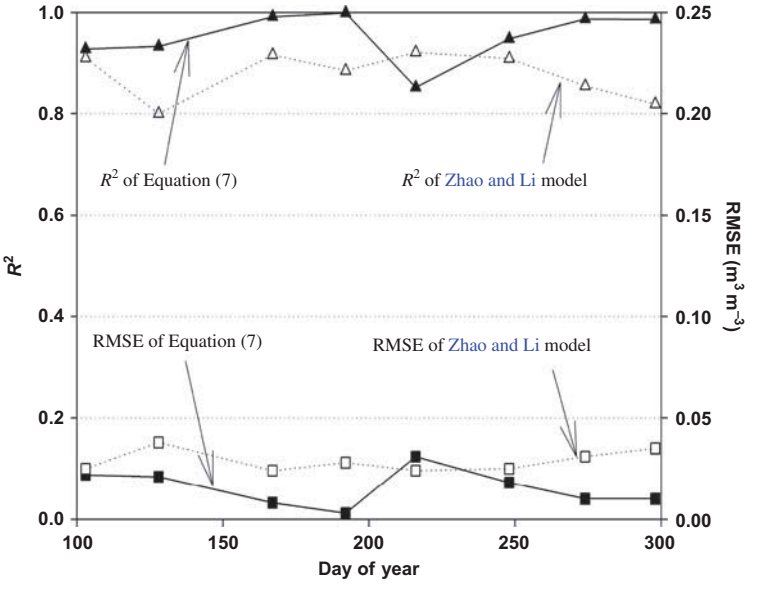

Figure 7. Comparison of R^2 and RMSE of the proposed SSM retrieval model and Zhao and Li's (2013) model for eight cloud-free days.

(2013) model also vary with different atmospheric conditions for each cloud-free day. Comparison of R^2 and RMSE of the two models is presented in Figure 7. As seen from this figure, both models can provide SSM with relatively high accuracy, but the model proposed in this paper is slightly more accurate overall.

3.4. *Validation with measured data*

To further assess the ability of Equation (7) to estimate SSM for bare soil, a preliminary validation was performed using the data measured at the two AmeriFlux sites, Bondville (40.0062° N, 88.2904° W) and Bondville Companion (40.0061° N, 88.2918° W). Since we are unable to acquire the model parameters n_i (i = 0, 1, 2, 3, 4) with the measured data available at these two sites, the land-surface model is used to obtain the model parameters n_i (i = 0, 1, 2, 3, 4) by simulation, as shown in Figure 1. With the simulation by CoLM, model parameters n_i (i = 0, 1, 2, 3, 4) of 14 typical cloud-free days in the year 2007 (DOY110, 127, 134, 141, 160, 213, 225, 243, 255, 256, 282, 302, 305, and 308) at the Bondville site, together with the ten typical cloud-free days in the years 2006 (DOY 297, 301, 302, and 313) and 2007 (DOY 302, 303, 305, 306, 308, and 313) at the Bondville Companion site, were obtained. Furthermore, ellipse parameters (x_0, y_0, a, b, and θ) for each of these cloud-free days were calculated by Equation (5) based on the measured diurnal LST and NSSR cycles. Finally, daily average SSM values were estimated with the simulated model parameters n_i (i = 0, 1, 2, 3, 4) and the fitted ellipse parameters (x_0, y_0, a, and θ) according to Equation (7). Figures 8 and 9 depict the measured and estimated daily average SSM for each site. Coefficients of determination R^2 = 0.548 with RMSE = 0.088 m^3 m^{-3} and R^2 = 0.445 with RMSE = 0.126 m^3 m^{-3} were achieved for the Bondville Companion site and the Bondville site, respectively. As seen from these figures, the trend observed in the estimated values is similar to that in the measured

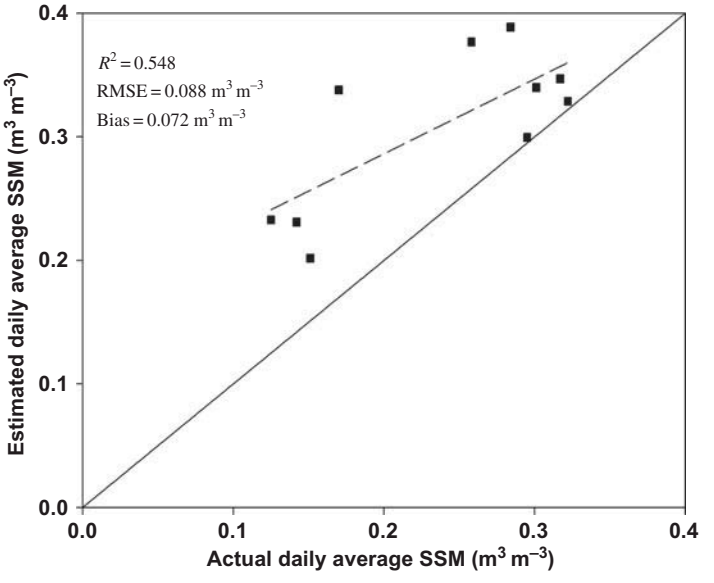

Figure 8. Scatter plots of the actual daily average SSM and the estimated average daily SSM of the ten cloud-free days at the Bondville Companion site.

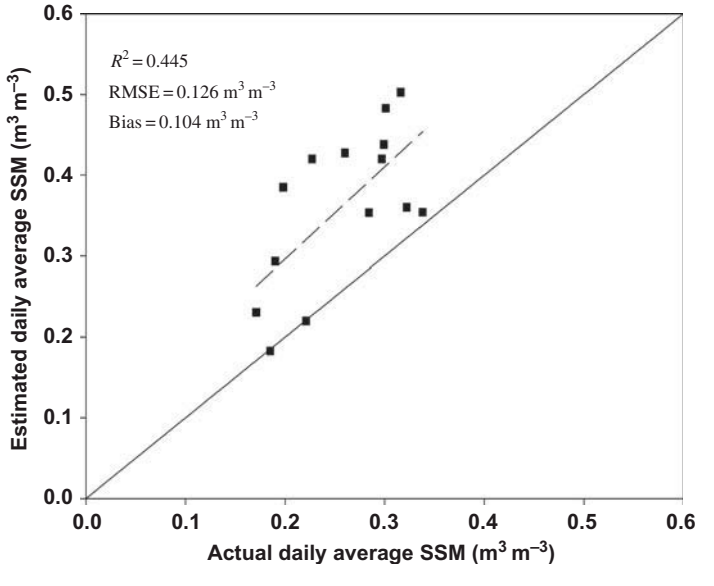

Figure 9. Scatter plots of the actual daily average SSM and the estimated average daily SSM of the 14 cloud-free days at the Bondville site.

average daily SSM, though the estimates are higher than the actual values. This over-estimation mainly occurs because the data simulation could not provide every aspect of the actual conditions. However, the relatively high coefficient of determination (R^2 = 0.548 or 0.445) indicates a better consistency between the estimated daily average SSM and the actual SSM values.

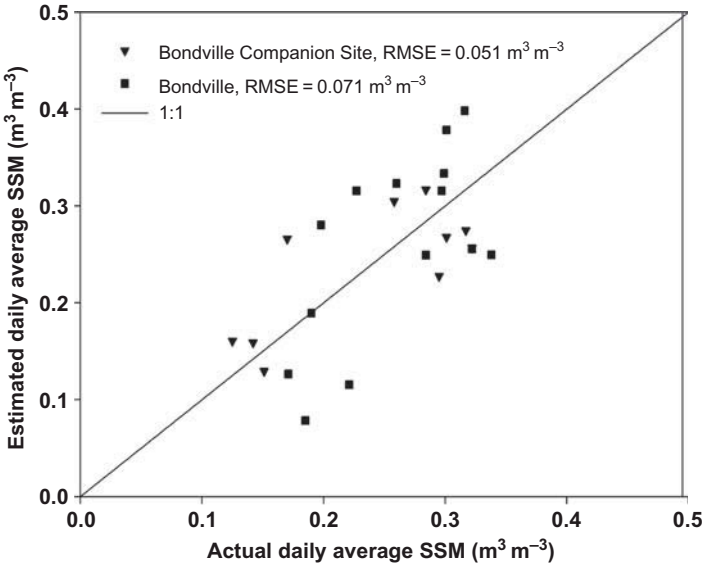

Figure 10. Scatter plots of the actual SSM and the estimated SSM of the cloud-free days for the two AmeriFlux sites; a simple calibration was conducted to adjust the Bias.

Finally, Bias = 0.072 m^3 m^{-3} was obtained and used to calibrate the estimated daily average SSM at Bondville Companion site, while Bias = 0.104 m^3 m^{-3} was recorded for the Bondville site. With this calibration processing, scatter plots of the measured daily average SSM and estimated values are shown in Figure 10. After calibration, RMSE of the estimated average daily SSM and the measured SSM significantly reduces from 0.088 m^3 m^{-3} to 0.051 m^3 m^{-3} for the Bondville Companion site, and from 0.126 m^3 m^{-3} to 0.071 m^3 m^{-3} for the Bondville site.

Validation results suggest that the proposed SSM retrieval model is capable of estimating daily average SSM with RMSE of approximately 0.051 m^3 m^{-3} at the Bondville Companion site, and 0.071 m^3 m^{-3} at the Bondville site. However, the estimated results are an over-estimation, and Bias is needed to calibrate the daily average SSM retrieval model. Theoretically, at least five field measurements with various soil types and SSM under a given atmospheric condition are needed to obtain the five model parameters n_i (i = 0, 1, 2, 3, 4) in Equation (7). Alternatively, the model parameters can also be achieved by a land-surface model simulation in the case of insufficient field measurements. However, data simulation can never fully describe the whole reality, and errors might also exist in the observed diurnal LST and NSSR cycles as well as the SSM values, which will lead to Bias between the estimated daily average SSM and actual values. Besides, SSM were measured in the top layer (0–10 cm) at the Bondville Companion site, while the estimated daily average SSM are related to a layer depth of 5 cm, and therefore the SSM values used in the validation also have a marginal influence on the accuracy of the proposed model.

3.5. *Further development*

Based on the simulated data, the proposed daily average SSM retrieval model proved to be capable of estimating SSM for bare surfaces, and a preliminary validation with field

measurements further verified its feasibilities. Because it is hard to find a satellite pixel without the presence of vegetation in natural surfaces (about 10 km^2), except for desert regions, remotely sensed data were not involved in the present study. In addition, as stated above, the five model parameters n_i (i = 0, 1, 2, 3, 4) in Equation (7) vary for different atmospheric conditions, and thus how to acquire these model parameters at the regional scale is another essential point that should be addressed before applying the proposed SSM model to remotely sensed data. Generally, these two points are the pivotal issues that concern the application of the model with remotely sensed observations, and they are also promising and being pursued as part of our future work. Besides, investigating the relationship between model parameters and atmospheric conditions is probably a promising avenue to making the SSM retrieval model more universal.

4. Conclusion

SSM is a key land surface variable in many applications and environmental studies. With the simulated data, a multi-linear model fully utilizing daytime LST and NSSR was developed to estimate daily average SSM. To develop the model, CoLM was selected to produce the data including diurnal LST and NSSR cycles as well as synergistic SSM variation. Based on the simulated data, a simple stepwise linear regression was performed to acquire the four ellipse parameters derived from the elliptical relationship between diurnal LST and NSSR cycles, thereby to develop the daily average SSM retrieval model. A good agreement was achieved using the average daily SSM retrieval model, with RMSE ranging from 0.003 to 0.031 $m^3\ m^{-3}$ and the coefficient of determination (R^2) ranging from 0.852 to 0.999 for the eight cloud-free days. Results showed that the coefficients of the model were independent of soil type and varied each day. To evaluate the proposed model, simulated data were used to compare our results to the SSM retrieval model developed by Zhao and Li (2013). Results indicated that the proposed model was more accurate. In addition to the simulated data, field measurements at the Bondville Companion site and Bondville site were also used to evaluate the model. Coefficients of determination R^2 = 0.548 and R^2 = 0.445 were achieved between the measured daily average SSM and the estimated values for these two sites, respectively, which indicated a better consistency between the estimated daily average SSM and the actual values. With a simple calibration to adjust the Bias, RMSE reduced from 0.088 $m^3\ m^{-3}$ to 0.051 $m^3\ m^{-3}$ at the Bondville Companion site, and from 0.126 $m^3\ m^{-3}$ to 0.071 $m^3\ m^{-3}$ at Bondville site.

According to this study, the proposed SSM retrieval model is capable of estimating daily average SSM, and the model parameters n_i (i = 0, 1, 2, 3, 4) are independent of soil type. However, the model parameters are strongly dependent on atmospheric conditions. As the development of the proposed SSM retrieval model for bare surfaces is based on simulated data, generally two points need to be considered before applying the model to geostationary satellite data in the future. The first is to take into account the vegetation in the SSM retrieval model, the second is how to obtain the five model parameters n_i (i = 0, 1, 2, 3, 4) at a regional scale. Besides, we will also focus on the relationship between the model parameter n_i (i = 0, 1, 2, 3, 4) and atmospheric conditions to make the model more universal.

Acknowledgement

The authors thank FLUXNET for supplying data and advice.

Funding

The work described in this articel was supported in part by the National Nature Science Foundation of China [grant number 41271379]; partly supported by the CAS (Chinese Academy of Sciences) Action-Plan for West Development [grant number KZCX2-XB3–15]; and also partly supported by the Exploratory Forefront Project for the Strategic Science Plan in IGSNRR, CAS [grant number 2012QY006]. Mr Pei Leng was financially supported by the China Scholarship Council for his stay at ICube, Strasbourg, France.

References

Chen, C., N. Son, L. Chang, and C. Chen. 2011. "Monitoring of Soil Moisture Variability in Relation to Rice Cropping Systems in the Vietnamese Mekong Delta Using MODIS Data." *Applied Geography* 31: 463–475.

Dai, Y., and D. Ji. 2008. *The Common Land Model (CoLM) User's Guide*. http://globalchange.bnu.edu.cn/research/models.

Entekhabi, D., and I. Rodriquez-Iturbe. 1994. "Analytical Framework for the Characterization of the Space-Time Variability of Soil Moisture." *Advances in Water Resources* 17: 35–45.

Fitzgibbon, A., M. Pilu, and R. B. Fisher. 1999. "Direct Least Square Fitting of Ellipses." *IEEE Transactions on Pattern Analysis and Machine Intelligence* 21: 476–480.

Gokmen, M., Z. Vekerdy, A. Verhoef, W. Verhoef, O. Batelaan, and C. Van der Tol. 2012. "Integration of Soil Moisture in SEBS for Improving Evapotranspiration Estimation under Water Stress Conditions." *Remote Sensing of Environment* 121: 261–274.

Göttsche, F., and F. Olesen. 2001. "Modelling of Diurnal Cycle of Brightness Temperature Extracted from METEOSAT Data." *Remote Sensing of Environment* 76: 337–348.

Idso, S., R. Jackson, R. Reginato, B. Kimball, and F. Nakayama. 1975. "The Dependence of Bare Soil Albedo on Soil Water Content." *Journal of Applied Meteorology and Climatology* 14: 109–113.

Jiang, G., Z.-L. Li, and F. Nerry. 2006. "Land Surface Emissivity Retrieval from Combined Mid-Infrared and Thermal Infrared Data of MSG-SEVIRI." *Remote Sensing of Environment* 105: 326–340.

Krishnan, P., A. Black, J. Grant, G. Barr, H. Hogg, S. Jassal, and K. Morgenstern. 2006. "Impact of Changing Soil Moisture Distribution on Net Ecosystem Productivity of Boreal Aspen Forest During and Following Drought." *Agricultural and Forest Meteorology* 139: 208–223.

Li, Z.-L., B.-H. Tang, H. Wu, H. Ren, G. Yan, Z. Wan, I. Trigo, and J. Sobrino. 2013. "Satellite-Derived Land Surface Temperature: Current Status and Perspectives." *Remote Sensing of Environment* 131: 14–37.

Li, Z.-L., R. Tang, Z. Wan, Y. Bi, C. Zhou, B.-H. Tang, G. Yan, and X. Zhang. 2009. "A Review of Current Methodologies for Regional Evapotranspiration Estimation from Remotely Sensed Data." *Sensors* 9: 3801–3853.

Li, Z.-L., H. Wu, N. Wang, S. Qiu, J. Sobrino, Z. Wan, B.-H. Tang, and G. Yan. 2013. "Land Surface Emissivity Retrieval from Satellite Data." *International Journal of Remote Sensing* 34 (9–10): 3084–3127.

Lu, N., J. Qin, K. Yang, and J. Sun. 2011. "A Simple and Efficient Algorithm to Estimate Daily Global Solar Radiation from Geostationary Satellite Data." *Energy* 36: 3179–3188.

Minacapilli, M., M. Iovino, and F. Blanda. 2009. "High Resolution Remote Estimation of Soil Surface Water Content by a Thermal Inertia Approach." *Journal of Hydrology* 379: 229–238.

Mintz, Y., and Y. Serafini. 1992. "A Global Monthly Climatology of Soil Moisture and Water Balance." *Climate Dynamics* 8: 13–27.

Patel, N., R. Anapashsh, S. Kuma, S. Saha, and V. Dadhwal. 2009. "Assessing Potential of MODIS Derived Temperature/Vegetation Condition Index (TVDI) to Infer Soil Moisture Status." *International Journal of Remote Sensing* 30: 23–39.

Pierdicca, N., L. Pulvirenti, and C. Bignami. 2010. "Soil Moisture Estimation over Vegetated Terrains Using Multitemporal Remote Sensing Data." *Remote Sensing of Environment* 114: 440–448.

Price, J. 1977. "Thermal Inertia Mapping: A New View of the Earth." *Journal of Geophysical Research* 82: 2582–2590.

Price, J. 1980. "The Potential of Remotely Sensed Thermal Infrared Data to Infer Surface Soil Moisture and Evaporation." *Water Resources Research* 16: 787–795.
Qian, B., R. Jong, and S. Gameda. 2009. "Multivariate Analysis of Water-Related Agroclimatic Factors Limiting Spring Wheat Yields on the Canadian Prairies." *European Journal of Agronomy* 30: 140–150.
Saha, S. 1995. "Assessment of Regional Soil Moisture Conditions by Coupling Satellite Sensor Data with a Soil-Plant System Heat and Moisture Balance Model." *International Journal of Remote Sensing* 16: 973–980.
Saltelli, A., S. Tarantola, F. Campolongo, and M. Ratto. 2004. *Sensitivity Analysis in Practice: A Guide to Assessing Scientific Models,* 217. Chichester: Wiley & Sons.
Schmugge, T., B. Blanchard, A. Anderson, and J. Wang. 1978. "Soil Moisture Sensing with Aircraft Observations of the Diurnal Range of Surface Temperature." *Journal of the American Water Resources Association* 14: 169–178.
Seneviratne, S., T. Corti, E. Davin, M. Hirschi, E. Jaeger, I. Lehner, B. Orlowsky, and A. Teuling. 2010. "Investigating Soil Moisture-Climate Interactions in Changing Climate: A Review." *Earth-Science Reviews* 99: 125–161.
Sobrino, J., and M. Romaguera. 2004. "Land Surface Temperature Retrieval from MSG1-SEVIRI Data." *Remote Sensing of Environment* 92: 247–254.
Song, X., P. Leng, X. Li, X. Li, and J. Ma. 2013. "Retrieval of Daily Evolution of Soil Moisture from Satellite-Derived Land Surface Temperature and Net Surface Shortwave Radiation." *International Journal of Remote Sensing* 34: 3289–3298.
Song, X., and Y. Zhao. 2006. "An Improved Method to Monitor Water Deficit in Regional Scale." *Science in China (Series D Earth Sciences*) 36: 188–194.
Szép, I., J. Mika, and Z. Dunkel. 2005. "Palmer Drought Severity Index as Soil Moisture Indicator: Physical Interpretation, Statistical Behaviour and Relation to Global Climate." *Physics and Chemistry of the Earth* 30: 231–243.
Tang, B.-H., Y. Bi, Z.-L. Li, and J. Xia. 2008. "Generalized Split-Window Algorithm for Estimate of Land Surface Temperature from Chinese Geostationary FengYun Meteorological Satellite (FY-2c) Data." *Sensors* 8: 933–951.
Verstraeten, W., F. Veroustraete, C. Sande, I. Grootaers, and J. Feyen. 2006. "Soil Moisture Retrieval Using Thermal Inertia, Determined with Visible and Thermal Spaceborne Data, Validated for European Forests." *Remote Sensing of Environment* 101: 299–314.
Wetzel, P., D. Atlas, and R. Woodward. 1984. "Determining Soil Moisture from Geosynchronous Satellite Infrared Data: A Feasibility Study." *Journal of Climate and Applied Meteorology* 23: 375–391.
Wetzel, P., and R. Woodward. 1987. "Soil Moisture Estimation Using GOES-VISSR Infrared Data: A Case Study with a Simple Statistical Method." *Journal of Climate and Applied Meteorology* 26: 107–117.
Xue, Y., and A. Cracknell. 1995. "Advanced Thermal Inertia Modeling." *International Journal of Remote Sensing* 16: 431–446.
Zhao, W., and Z.-L. Li. 2013. "Sensitivity Study of Soil Moisture on the Temporal Evolution of Surface Temperature over Bare Surfaces." *International Journal of Remote Sensing* 34: 3314–3331.
Zhao, W., Z.-L. Li, H. Wu, B.-H. Tang, X. Zhang, X. Song, and G. Zhou. 2013. "Determination of Bare Surface Soil Moisture from Combined Temporal Evolution of Land Surface Temperature and Net Surface Shortwave Radiation." *Hydrological Process.* doi:10.1002/hyp.9410.